

Microbunch Instability in the Beijing XFEL Test Facility Bunch Compressor^{*}

YANG Yu-Feng^{1;1)} ZHU Xiong-Wei¹ LI Ming²

1 (Institute of High Energy Physics, CAS, Beijing 100049, China)

2 (Institute of Applied Electronics of CAEP, Mianyang 621900, China)

Abstract We numerically studied the microbunch instability driven by Coherent synchrotron radiation (CSR) in a magnet bunch compressor. High-frequency density perturbation may be significantly amplified when an electron beam passes through the Beijing XFEL Test Facility (BTF) magnet bunch compressor II. The dependence of CSR-driven microbunch instability on bunch twiss parameters is sensitive. Dangerous area of twiss parameters is outlined.

Key words microbunch instability, coherent synchrotron radiation, compressor, twiss parameter

1 Introduction

Microbunch instability induced by coherent-synchrotron-radiation (CSR) in the bunch compressor was highlighted in recent years^[1–5]. Such an instability was studied on several famous facilities, including LCLS^[1] and DESY^[6, 7]. The studies revealed that CSR of a bunch in a bunch compressor may lead to the microwave instability producing longitudinal modulation of the bunch with wavelengths which are small compared to the bunch length^[8]. Theoretically, S. Heifets^[4] first brought a 3-dimensional model for CSR-driven microbunch instability, which took into account the transverse motion of the beam neglected before. With the model, S. Heifets studied the CSR-driven microbunch instability in the LCLS compressor, where the microwave perturbation whose wavelengths lie between 20–50 micrometers generated notable instability. On the above basis, this paper aims at two issues: First, can the CSR-driven microbunch instability occur in the newly proposed Beijing XFEL Test Facility (BTF)^[9] compressor and is it strong?

Second, what is the dependence of the CSR-driven microbunch instability on bunch quality?

We organize the paper as follows. First, we review the microbunch theory and introduce our numerical methods. After that, we show our studies of the CSR-driven microbunch instability. Finally, we draw a brief conclusion and conduct discussion.

2 Theoretical basis and numerical methods

From a linear Vlasov equation, S. Heifets derived the amplification of a high-frequency density perturbation of the electron beam in a bunch compressor. Below we take a brief review for S. Heifets' theory^[4].

Consider an electron beam whose velocity is around light-velocity c . Of all the electrons, the one with normal energy follows a trajectory s , $s = ct$ where t is the time. We define s as the reference trajectory of all trajectories. The reference trajectory in a magnet compressor consists of alternate circular-linear orbits, with circular radius R . The longitudinal coordinate of any other electron trajectory mea-

Received 17 April 2006, Revised 23 June 2006

^{*} Supported by NSFC (10575114) and National Laboratory of High Power Radiation Found (20040302)

1) E-mail: yfyang@mail.ihep.ac.cn

sured to the reference trajectory is denoted by z , and the horizontal offset is denoted by x . Suppose the beam emittance at entrance is ε_0 ; the uncorrelated energy spread is σ_p ; the beta function is $\beta(s)$, with $\beta(s) = w(s)^2$ and $w(s)$ satisfying $w(s)'' = 1/w(s)^3$; the alfa function is $\alpha(s)$, with $\alpha(s) = -\frac{d\beta(s)}{2ds}$; the dispersion function is D , with D satisfying $D(s)'' = 1/R(s)$. Then, we can get $R_{51}(s)$, $R_{52}(s)$, $R_{56}(s)$ and betatron phase $\varphi(s)$ ^[4]:

$$R_{51}(s) = -\frac{1}{\sqrt{\beta_0}} \int_0^s \frac{\sqrt{\beta(s')}}{R(s')} \cos \varphi(s') ds', \quad (1)$$

$$R_{52}(s) = -\sqrt{\beta_0} \int_0^s \frac{\sqrt{\beta(s')}}{R(s')} \sin \varphi(s') ds', \quad (2)$$

$$R_{56}(s) = \int_0^s \frac{D(s')}{R(s')} ds', \quad (3)$$

$$\varphi(s) = \int_0^s \frac{ds'}{\beta(s')}. \quad (4)$$

Then, the compression factor $C(s)$ is obtained with $C(s) = \frac{1}{1 - uR_{56}(s)}$, where u is the longitudinal slope of energy spread at entrance of the compressor. Suppose the high-frequency density perturbation has wavelength λ , wave number k being $k = 2\pi/\lambda$; the equilibrium density is $n_0(s, z)$; the perturbation amplitude is $n_{1,k}(s, z)$. Evidently, the initial perturbation amplitude at entrance is $n_{1,k}(0, z)$. S. Heifets proved that $n_{1,k}(s, z)$ can be written as:

$$n_{1,k}(z, s) = C(s)g_k(s)e^{ikC(s)z}. \quad (5)$$

Where $g_k(s)$ is defined as Eq. (6):

$$g_k(s) = g_k^0(s) + \int_0^s K(s, s')g_k(s')ds'. \quad (6)$$

Where $g_k^0(s)$ is:

$$g_k^0(s) = n_{1,k}(0, z) \times e^{-[C(s)^2 k^2 \varepsilon_0 / 2\beta(0)] [\beta(0)^2 R_{51}(s)^2 + R_{52}(s)^2] - C(s)^2 k^2 \sigma_p^2 R_{56}(s)^2 / 2} \quad (7)$$

and $K(s, s')$ in Eq. (6) is calculated through Eq. (8):

$$K(s, s') = \frac{ikr_e n_b}{\gamma} C(s)C(s')Z(kC(s'), s')R_{56}(s' \rightarrow s) \times e^{-[k^2 \varepsilon_0 / 2\beta(0)] [\beta(0)^2 R_{51}(s, s')^2 + R_{52}(s, s')^2] - k^2 \sigma_p^2 R_{56}(s, s')^2 / 2}. \quad (8)$$

In Eq. (8), $R_{51}(s, s')$, $R_{52}(s, s')$, $R_{56}(s, s')$ and $R_{56}(s' \rightarrow s)$ are defined as below^[4] (Note that

$R_{56}(s' \rightarrow s)$ is only a symbol to replace below Eq. (12) for short):

$$R_{51}(s, s') = C(s)R_{51}(s) - C(s')R_{51}(s'), \quad (9)$$

$$R_{52}(s, s') = C(s)R_{52}(s) - C(s')R_{52}(s'), \quad (10)$$

$$R_{56}(s, s') = C(s)R_{56}(s) - C(s')R_{56}(s'). \quad (11)$$

$$R_{56}(s' \rightarrow s) = -\int_{s'}^s \frac{ds_1}{R(s_1)} \int_{s'}^s \frac{ds_2}{R(s_2)} \sqrt{\beta(s_1)\beta(s_2)} \times \sin[\varphi(s_1) - \varphi(s_2)]. \quad (12)$$

Other symbols in Eq. (8): γ represents the relative energy factor; $r_e = 2.8 \times 10^{-15} \text{m}$ is the classical electron radius; $Z(k, s) = -i \frac{k^{1/3}(1.63i - 0.94)}{R(s)^{2/3}} \times \frac{Z_0}{4\pi}$ ($Z_0 = 377\Omega$) is the CSR wake impedance^[10]; n_b is the number of electrons per unit length at entrance.

The normalized amplification factor for the high-frequency density perturbation of the microbunch can be defined as:

$$G(s) = \frac{n_{1,k}(s, z)}{C(s)n_{1,k}(0, z)} = |g_k(s)|. \quad (13)$$

It measures the CSR-driven microbunch instability.

To get $g_k(s)$, $\beta(s) = w(s)^2$ should be first calculated. To deal with $w(s)'' = 1/w(s)^3$ where the initial values of $w(0), w'(0)$ are given, we use a numerical method which greatly reduces the iteration process. Divide the reference trajectory into N sections, each section length $d = s/N$. The start point of the first section is denoted by point 0, and the end of each section is denoted by points 1, 2, \dots i \dots N in sequence. The w values at points 1, 2, \dots i \dots N are $w_1, w_2, \dots, w_i, \dots, w_N$. The following can be easily got:

$$\left. \begin{aligned} w'_i &= \frac{w_{i+1} - w_{i-1}}{2d}, \\ w''_i &= \frac{w'_{i+1/2} - w'_{i-1/2}}{d} = \frac{w_{i+1} + w_{i-1} - 2w_i}{d^2} = \frac{1}{w_i^3} \end{aligned} \right\} \Rightarrow$$

$$\left\{ \begin{aligned} w_{i+1} - w_{i-1} &= 2dw'_i \\ w_{i+1} + w_{i-1} &= \frac{d^2}{w_i^3} + 2w_i \end{aligned} \right\} \Rightarrow w_{i+1} = w_i + dw'_i + \frac{d^2}{2w_i^3}, \quad (14)$$

where the subscript $i+1/2$ denotes the point $d/2$ behind point i and the subscript $i-1/2$ denotes the point $d/2$ in front of point i . We see that $w_{i+1/2}, w_{i-1/2}$ vanish during the derivation. Through Eq. (14), w' values

of the next point $i+1$, can be calculated with w, w' values of current point i . Iteratively applying (14) from $i=0$ to $N-1$, $\beta(s)$ can be obtained. Though simple, the method gives rather consistent results when N adopts 100 and 400, which differs by less than 1%.

Secondly, we should calculate the function $K(s, s')$ based on Eq. (8), which is a $N \times N$ matrix $K(i, j)$ here. For Eq. (8), the term $R_{56}(s' \rightarrow s)$ dominates most of the calculating time. If we directly calculate $R_{56}(s' \rightarrow s)$ using Eq. (12), the calculating time of the whole matrix $K(i, j)$ is proportional to N^4 , maybe several days for $N \sim 400$. Using the following relation:

$$R_{56}(s' \rightarrow s+d) = R_{56}(s' \rightarrow s) + \int_{s'}^{s+d} \frac{d \cdot ds_1}{R(s+d)R(s_1)} \times \sqrt{\beta(s+d)\beta(s_1)} \sin[\varphi(s+d) - \varphi(s_1)], \quad (15)$$

the calculation time can be reduced to $\propto N^3$, only several minutes for $N \sim 400$.

With this method, we built up a computer code to calculate $g_k(s)$. The results will be shown in the next part.

3 Results and analysis

We applied the above method to the Beijing XFEL Test Facility magnet compressor II, which has four dipole magnets and three drift sections. Its total length is 7.77m; the distance between the middle two magnets is 0.17m; each magnet is 0.2m long and generates a circular particle trajectory whose radius is 3.18m. At this position, the beam energy reaches to 0.705GeV. The longitudinal slope of energy spread $u = -32.6\text{m}^{-1}$. The horizontal normalized beam emittance is $1.43\mu\text{m}$. $n_b = 1.7e^{12}\text{m}^{-1}$ and $\sigma_p = 3e^{-5}$. The dispersion function of $D(s)$, and $R_{56}(s)$ is shown in Fig. 1.

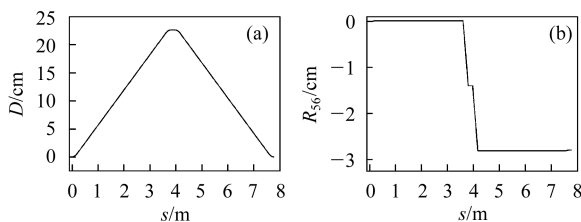


Fig. 1. The curve of $D(s)$ and $R_{56}(s)$.

As defined in Eq. (13), $G(s)$ describes the amplification of the high-frequency density perturbation of the microbunch. The change of $G(s)$ along the reference trajectory is shown in Fig. 2, calculated at four different $\lambda - \beta_0 - \alpha_0$ parameter-groups. We see that $G(s)$ can exceed 1 at the compressor end when the perturbation wavelength $\lambda = 50\mu\text{m}$, indicating the existence of microbunch instability. While $G(s)$ approaches 0 finally when $\lambda = 10\mu\text{m}$, indicating that the perturbation vanishes and has no impact on the microbunch. Thus, the perturbation frequency should be a sensitive factor for microbunch density modulation.

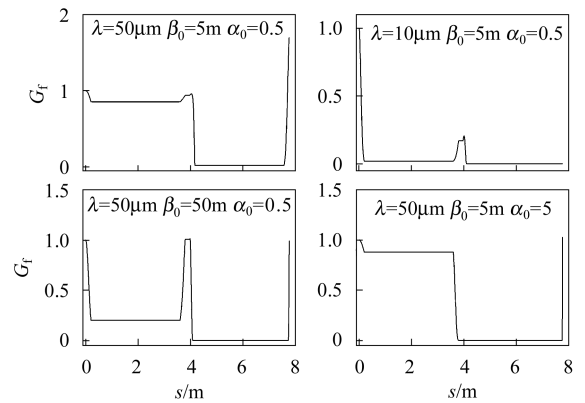


Fig. 2. The evolution of $G(s)$ along s at different parameters.

We calculated the dependence of amplification factor G on perturbation wavelength λ , as Fig. 3 shows. The final value of $G(s)$ at the compressor end is denoted by G_f . We see that the very-high frequency perturbation whose wavelength is less than $20\mu\text{m}$ has no modulation for the microbunch. As the perturbation wavelength increases to be comparable with the microbunch length ($\sim 140\mu\text{m}$), the density modulation becomes significant. However, if the

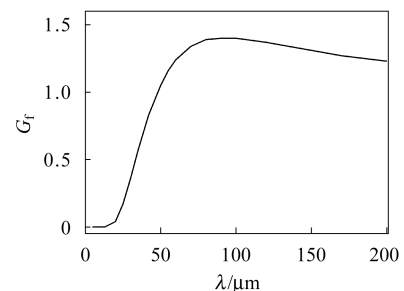


Fig. 3. The dependence of G_f on λ at typical twiss parameters $\beta_0=43\text{m}$, $\alpha_0=1.77$.

perturbation wavelength is too long, the modulation is also reduced. Such a result agrees with previous findings^[4].

We also studied the dependence of density modulation on microbunch parameters, i.e., twiss parameters β_0 and α_0 (Figs. 4—6). The relation between G_f and β_0 is shown in Fig. 4. We see that G_f - β_0 relation is nonlinear and G_f peaks at specific β_0 values. The non-linearity is reasonable according to Eqs. (3)—(5). The peak positions of G_f in Fig. 4 are usually located at several meters of β_0 , indicating that small transverse-distributing of microbunch may bring significant density modulation and instability. It is interesting that two peaks can appear in one G_f - β_0 curve when α_0 adopts some value (i.e, $\alpha_0=5$ here). These suggest that the dependence of amplification factor G_f on twiss parameters is complex and requires careful computation.

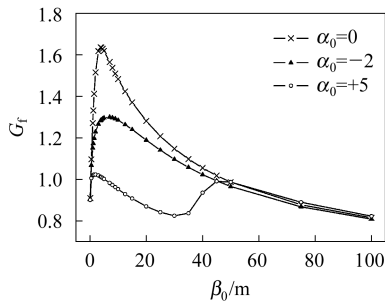


Fig. 4. The dependence of G_f on β_0 at $\lambda=50\mu\text{m}$.

Fig. 5 exhibits the G_f - α_0 relation. Non-linearity exists too. At each curve, G_f maximizes when α_0 approaches 0. When α_0 departs from 0 values, whether it increases or decreases, G_f uniquely decreases.

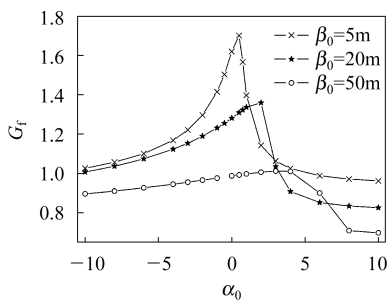


Fig. 5. The dependence of G_f on α_0 at $\lambda=50\mu\text{m}$.

In Figs. 4—5, when β_0 - α_0 adopts different typical values, the maximal G_f reaches 1.7 and the minimal G_f is only 0.7. According to Eq. (5), the up-

per phenomenon implies that the microbunch density modulation differs greatly when the twiss parameters are adjusted (the compress factor $C(s)$ should be also taken into account).

We made a lot of calculations for G_f at different twiss-parameters, β_0 changing between 1—50m, α_0 between -5 — $+5$, to draw the dependence of G_f on β_0 - α_0 , as Fig. 6 shows. Fig. 6 plots the contour lines of G_f in a β_0 - α_0 plane. $G_f > 1$ in the major twiss-parameter area, implying that commonly the microbunch perturbation will be amplified in BTF magnet bunch compressor II when the perturbation wavelength is comparable with the bunch length. The largest amplification appears near $\alpha_0 \sim 0$ — 0.5 , agreeing with Fig. 5.

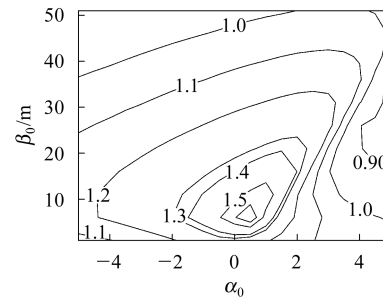


Fig. 6. G_f contour lines on β_0 - α_0 plane at $\lambda=50\mu\text{m}$.

4 Conclusion and discussion

We numerically studied the microbunch density modulation in a magnet compressor induced by CSR effect. We apply our study to the newly proposed Beijing XFEL Test Facility(BTF). Numerical results reveal that the microbunch instability will usually emerge when beam passes through BTF compressor II. However, a too high or too low frequency of perturbation brings no danger to microbunch. Only when the perturbation wavelength reaches around the microbunch length, perturbation amplification will be observable. For BTF, the specific perturbation length is about $100\mu\text{m}$, longer than 20 — $50\mu\text{m}$ of LCLS^[4]. Evidently, this is because BTF has lower beam energy than LCLS.

An important theme of this paper is that we first explored the sensitive dependence of perturbation

amplification on bunch twiss parameters. The dependence maintains significant non-linearity. The amplification factor maximizes at specific twiss parameters, i.e., near $\alpha_0 \sim 0-0.5$. Small traverse beam section

seems to inspire large amplification factor. The relation between microbunch instability and bunch quality is complex and we presented the careful calculations (Fig. 6).

References

- 1 The LCLS Design Study Group. SLAC Report, SLAC-R-521, 1998
- 2 Heifets S, Stupakov G. SLAC Report, SLUC-PUB-8988, 2001
- 3 Saldin E L, Schneidmiller E A, Yurko M V. DESY Report, TELSAs-FEL-2002-02, 2002
- 4 Heifets S, Stupakov G. Phys. Rev. ST Accel. Beams, 2002, **5**: 064401
- 5 HUANG Zhi-Rong, Kim Kwang-Je. Phys. Rev. ST Accel. Beams, 2002, **5**: 074401
- 6 Saldin E L, Schneidmiller E A, Yurkov M V. NIM, 2001, **A475**: 353
- 7 Saldin E L, Schneidmiller E A, Yurkov M V. NIM, 2002, **A483**: 516
- 8 Heifets S, Stupakov G. SLAC Report, 2001, SLUC-PUB-8761
- 9 ZHU Xiong-Wei et al. High Energy Physics and Nuclear Physics, 2006, **30**(Suppl. I): 126
- 10 Murphy J B, Krinsky S, Gluckstern R L. Part. Accel., 1997, **57**: 9

北京 X 射线自由电子激光试验装置 (BTF) 磁压缩器中 微束团不稳定性的研究*

杨宇峰^{1;1)} 朱雄伟¹ 黎明²

1 (中国科学院高能物理研究所 北京 100049)

2 (中国工程物理研究院应用与电子学研究所 绵阳 621900)

摘要 用数值方法研究了相干同步辐射 (CSR) 引发的微束团不稳定性. 当电子通过北京 X 射线自由电子激光实验装置 (BTF) 的第二个磁压缩段时, CSR 调制将使微束团失稳. 这一不稳定性敏感的依赖于微束团 twiss 参数. 计算了不稳定的参数区.

关键词 微束团不稳定性 相干同步辐射 压缩器 twiss 参数

2006 - 04 - 17 收稿, 2006 - 06 - 23 收修改稿

* 国家自然科学基金(10575114)和国家863计划强辐射重点实验室(20040302)资助

1) E-mail: yfyang@mail.ihep.ac.cn